Langmuir

Article

pubs.acs.org/Langmuir

Formation of Carboxy- and Amide-Terminated Alkyl Monolayers on Silicon(111) Investigated by ATR-FTIR, XPS, and X-ray Scattering: Construction of Photoswitchable Surfaces

Karola Rück-Braun,*[,†] Michael Åxman Petersen,[†,∥] Fabian Michalik,[†] Andreas Hebert,[†] Daniel Przyrembel,[‡] Christopher Weber,[§] Saleh A. Ahmed,[†,⊥] Stefan Kowarik,[§] and Martin Weinelt*[,‡]

[†]Institut für Chemie, Technische Universität Berlin, Strasse des 17. Juni 135, 10623 Berlin, Germany

[‡]Fachbereich Physik, Freie Universität Berlin, Arnimallee 14, 14195 Berlin, Germany

[§]Institut für Physik, Humboldt-Universität zu Berlin, Newtonstrasse 15, 12489 Berlin, Germany

Supporting Information

ABSTRACT: We have prepared high-quality, densely packed, self-assembled monolayers (SAMs) of carboxy-terminated alkyl chains on Si(111). The samples were made by thermal grafting of methyl undec-10-enoate under an inert atmosphere and subsequent cleavage of the ester functionality to disclose the carboxylic acid end-group. X-ray photoelectron spectroscopy (XPS) and grazing incidence X-ray diffraction (GIXD) indicate a surface coverage of about 50% of the initially H-terminated sites. In agreement, GIXD implies a rectangular unit mesh of 6.65 and 7.68 Å side lengths, containing two molecules in a regular zigzag-like substitution pattern for the ester- and carboxy-terminated monolayer. Hydrolysis of the remaining H−Si(111) bonds at the surface furnished HO−Si(111) groups according to XPS and attenuated total reflection Fourier-transform infrared spectroscopy (ATR-FTIR) studies. The amide-terminated alkyl SAM on Si(111) assembled in a 2-(6-chloro-1*H*-benzotriazol-1-yl)-1,1,3,3-tetramethyluronium hexafluorophosphate (HCTU)-mediated one-pot coupling reaction under an inert atmosphere, whereby the active ester forms in situ prior to the reaction with an amino-functionalized photoswitchable fulgimide. ATR-FTIR and XPS studies of the fulgimide samples revealed closely covered amide-terminated SAMs. Reversible photoswitching of the headgroup was read out by applying XPS, ATR-FTIR, and difference absorption spectra in the mid-IR. In XPS, we observed a reversible breathing of the amide/imide C1s and N1s signals of the fulgimide. The results demonstrate the general suitability of HCTU as a reagent for amide couplings to carboxy-terminated alkyl SAMs and the on-chip functionalization toward photoswitchable Si(111) surfaces.

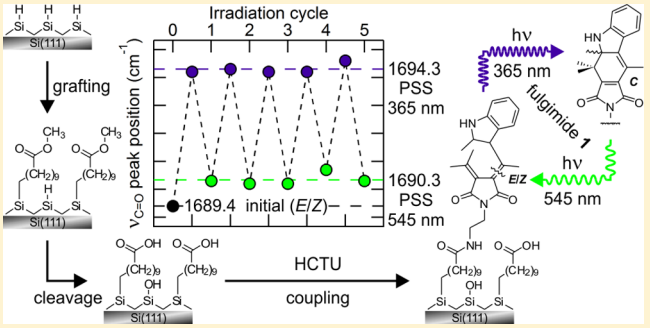

INTRODUCTION

Silicon is one of the most relevant materials for nanotechnology and semiconductor devices. In these fields, fine-tuning of the surface properties by well-defined organic molecules is of importance.[2,3] We are interested in on-chip synthetic routes for the assembly of organic molecules at semiconductor surfaces for biosensors and nanotechnology. Progress strongly depends on a high and reproducible quality of functionalized-alkyl self-assembled monolayers (SAMs). For these aims and purposes, a considerable number of wet-chemical multistep procedures starting from H-terminated Si(111) have been reported in the past decade.[4−6] Avoiding SAM oxidation is a major challenge during grafting and subsequent steps. Thus, the conditions for predictable and reproducible multistep transformations of terminal functional groups at the organic−semiconductor hybrid interface at ambient conditions have to be carefully chosen. The formation of active esters of *N*-hydroxysuccinimide (NHS) in an independent step is an extensively studied activation principle for carboxy-terminated alkyl SAMs prior to amide coupling.[6,7] NHS-terminated alkyl SAMs can be purified and stored over time. As a drawback, unreacted NHS groups have to be capped after amide coupling prior to subsequent transformations and applications, e.g., with ethanolamine.[5,6]

Only a few alternative protocols have been published, e.g., the use of trifluoroacetic anhydride and triethylamine furnishing anhydride-terminated monolayers prior to the formation of amide-terminated alkyl SAMs.[5] In peptide chemistry, in situ activation of carboxylic acids using aminium salts for amide coupling, e.g., HBTU or HCTU,[1] is common practice.[8] These coupling reagents effect the formation of an active ester intermediate that then undergoes aminolysis. This approach has the advantage of providing the amide-terminated alkyl SAM in one step without the need to monitor or to isolate and characterize reaction intermediates.

Received: May 30, 2013
Revised: July 24, 2013
Published: August 23, 2013

In this paper, we report on a HCTU protocol for the one-pot coupling of amines to carboxy-terminated alkyl SAMs on Si(111). The latter resulted from thermal grafting of a methyl ester-terminated SAM and subsequent on-chip cleavage. The reproducibility and quality of the SAMs were improved by performing the grafting step and the amide coupling in a closed vessel in a glovebox. All steps were analyzed by attenuated total reflection Fourier-transform infrared spectroscopy (ATR-FTIR) and X-ray photoelectron spectroscopy (XPS). X-ray scattering methods were applied for analyzing the ester- and the carboxy-terminated alkyl SAMs. Photochemical studies were carried out by alternating irradiation of the fulgimide samples with ultraviolet (UV) and visible light and readout by ATR-FTIR and XPS. Fulgimide **1** is most suitable for these studies, since strong changes of its vibrational modes are observed following the ultrafast ring-closure and ring-opening reactions.[9,10]

EXPERIMENTAL SECTION

General Remarks. Samples for X-ray photoelectron spectroscopy (XPS) and X-ray scattering were cut from single side polished Si(111) (Silchem, n-type, 7.5 Ω cm, thickness 525 μm) in 1 cm × 4 cm pieces. After each synthesis step a 1 cm × 1 cm sample was broken off from the main sample and transferred into the XPS or X-ray scattering apparatus. Samples for attenuated total reflection Fourier-transform infrared spectroscopy (ATR-FTIR) were cut from double side polished Si(111) (Siltronix, n-type, 10−30 Ω cm, thickness 500−550 μm) in 1.1 cm × 2.5 cm dimension, and the sides were cut and polished at an angle of 45°.

Methyl undec-10-enoate (97%) was purchased from Sigma-Aldrich, distilled twice under reduced pressure (124 °C, 14 mbar), and stored in a glovebox (MBraun, Labmaster). Ammonium sulfite [$(NH_4)_2SO_3 \cdot H_2O$], HCTU,[1] Hünig's base (diisopropylethylamine, biotech grade), and acetonitrile (amine-free) were purchased from Sigma-Aldrich and used without further purification. Hydrogen peroxide (H_2O_2, 31%), sulfuric acid (H_2SO_4, 96%), and ammonium fluoride (NH_4F, 40%) were of VLSI grade (very large scale integration grade, trace metal content <100 ppb) and purchased from BASF. Ultrapure Milli-Q water (18 MΩ cm) was obtained from a MilliPore four-bowl system.

Monolayer Preparation. The Si(111) wafers were cleaned by successive sonication in acetone, dichloromethane (DCM), and methanol, followed by treatment with "piranha" solution (H_2O_2/H_2SO_4, 1/3, v/v) for 30 min at 100 °C and then copiously rinsed with Milli-Q water. *CAUTION*: "piranha" solution reacts violently with organic material and must be handled with extreme care! The wet sample was directly transferred into the etching solution (40% NH_4F containing 50 mM $(NH_4)_2SO_3$).[11] After 15 min of etching the sample was quickly rinsed with ultrapure water and dried in a vacuum. Grafting was conducted in pure methyl undec-10-enoate in a closed vessel at 160 °C for 2 h in the glovebox. After cooling to room temperature, the sample was rinsed with hexane and DCM. The methyl ester in the monolayer was cleaved using 5.5 M hydrochloric acid (HCl) (degassed with argon) at 40 °C for 3 h followed by washing with ultrapure water and DCM.

Fulgimide Coupling. The carboxy-terminated surface was immersed in the glovebox for 2 h in the dark in a solution of an 85:15 mixture of (*E*/*Z*)-fulgimide [(*E*/*Z*)-**1**] (5 mM), HCTU (as coupling agent, 10 mM), and Hünig's base (10 mM) in acetonitrile. After the reaction, the samples were rinsed five times with 3 mL of acetonitrile and two times with 3 mL of DCM, blown dry, and stored under argon.

ATR-FTIR Measurements. The spectra were recorded with a Bruker Vertex70v ATR-FTIR spectrometer containing a liquid nitrogen-cooled mercury−cadmium−telluride (MCT) detector while the sample compartment was kept under a nitrogen atmosphere. The nitrogen to purge the spectrometer was dried with an absorption drier (Specken Drumag SDAT-G70/420) to contain less than 0.1 ppm water. We investigated the spectral range between 370 and 4000 cm^{-1} with 4 cm^{-1} resolution. Freshly prepared H-terminated Si(111) or SiO_x samples were used as references, as indicated in the text. IR data were analyzed using the software OPUS 6.5 (Bruker).

XPS Measurements. We used an XPS setup in an ultrahigh vacuum (UHV) mu-metal chamber equipped with a monochromatized Al KαI X-ray source (VG Scienta MX650; $h\nu$ = 1486.7 eV, 15 kV, 450 W) and a hemispherical electron analyzer (VG Scienta SES-200). After preparation of the various SAMs, samples were transported in an inert atmosphere and transferred into the UHV system via a quick-load lock.

XP spectra were recorded with an overall energy resolution of 0.4 eV. A takeoff angle of the photoelectrons of 65° with respect to the sample normal was chosen to enhance the surface sensitivity of the XPS measurements. In this geometry, the X-ray source features a line focus of about 3 mm × 9 mm, which helps to reduce radiation damage of the molecular layer below the detection limit. The setup has a typical operational pressure of 2 × 10^{-10} mbar, ensuring that surface contamination by residual gas adsorption is kept at a minimum during prolonged measurements. All spectra were measured at room temperature. For the quantitative XPS analyses, Shirley backgrounds were subtracted and the spectra fitted with Voigt profiles. To get out of the fits the peak positions of the amidic carbons in the fulgimide layers with reasonable errors, all other fit peaks were subtracted from the respective spectra and the remaining single peak spectrum fitted again with a Voigt profile (cf. Supporting Information, Figure S20).

XRR and GIXD Measurements. All X-ray reflectivity and diffraction measurements were performed using a lab-based diffractometer (EFG) with a Cu Kα (λ = 1.54 Å) rotating anode source (Rigaku). To prevent ozone exposure, the sample was kept in a vacuum ($p \approx 1$ mbar) during X-ray measurements. To exclude beam damage, the X-ray reflectivity (XRR) was repeatedly measured at several different spots on the sample. No changes due to X-ray exposure have been found. For XRR, the angular resolution was 0.05°, and the diffusely scattered signal, as determined by an offset scan, was subtracted from the raw XRR data to arrive at the true specular reflectivity. For the quantitative analysis of the XRR measurements, the specular reflectivity was fitted using a least-squares routine (Parratt32, Helmholtz-Zentrum Berlin) based on the Parratt algorithm.[12] The angular resolution of the grazing incidence X-ray diffraction (GIXD) scans was 0.3° at an angle of incidence of 0.18°.

Photoinduced Switching. For photoswitching, the SAMs were irradiated in the sample compartment of the ATR-FTIR spectrometer under nitrogen. Illuminated samples were then measured by ATR-FTIR or transferred in the dark under argon to the XPS setup. Using custom-made setups of light-emitting diodes with wavelengths of 365 and 545 nm at intensities of 2 and 5 mW cm^{-2}, the two photostationary states (PSS) were reached within 30 min of irradiation. This corresponds to a relatively small fluence of less than 10 J cm^{-2}.

Fulgimide Synthesis and Characterization. Indolylfulgimide **1** (Scheme 1) was synthesized in three steps starting from fulgide **5**, which was obtained essentially by following the route of Yokoyama et al.;[13] all intermediates were fully characterized. Tosylation of indole **2** furnished compound **3** in 90% yield. The Stobbe condensation of indole **3** with diethyl isopropylidenesuccinate was carried out with lithium diisopropylamide (LDA) as base and gave the monoester (*E*/*Z*)-**4** in 63% yield. Saponification of the monoester (*E*/*Z*)-**4** with hot aqueous ethanolic potassium hydroxide (KOH) solution gave the crude diacid. Subsequent anhydride formation with dicyclohexylcarbodiimide (DCC) afforded fulgide **5** as an 85:15 (*E*/*Z*)-mixture in 86% yield over the two steps after workup and purification by flash chromatography. Ring-opening of fulgide **5** with *tert*-butyl 2-aminoethylcarbamate in DCM gave the regioisomeric succinamic acids as an inseparable mixture that was treated with carbonyldiimidazole (CDI) in a one-pot procedure for the final imide ring closure. Fulgimide (*E*/*Z*)-**6** was isolated after workup and purification in 80% yield over the two steps. Deprotection with 4 M HCl in dioxane gave (*E*/*Z*)-**1** in 81% yield after aqueous basic workup and purification by flash-chromatography as an 85:15 mixture of the (*E*/*Z*)-forms used in the present studies. Compound **1a** was isolated as byproduct in 5% yield because of an acid-catalyzed carbonyl−ene

dx.doi.org/10.1021/la402068d | *Langmuir* 2013, 29, 11758−11769

Scheme 1[a]

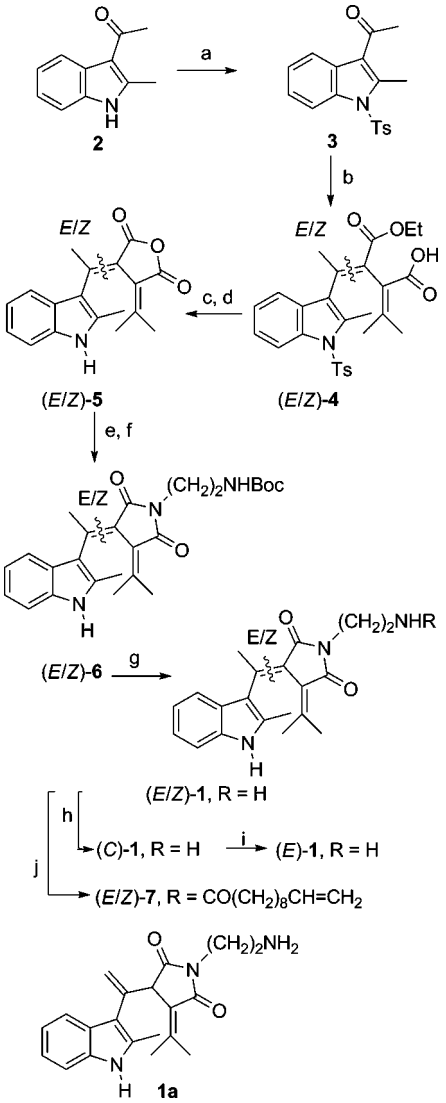

[a]Reagents and conditions: (a) TsCl, NaOH, DCM; 90%. (b) Diethyl isopropylidenesuccinate, LDA, THF; 63%. (c) KOH/EtOH/H_2O, reflux; 97%. (d) DCC, DCM; 86%. (e) *tert*-Butyl 2-aminoethylcarbamate, DCM, reflux and then (f) CDI; one-pot procedure, 80%. (g) 4 M HCl in dioxane; 81%. (h) 365 nm, benzene; 45%. (i) 545 nm, benzene; quant. (j) HCTU, undec-10-enoic acid, DIEA, acetonitrile; 96%.

reaction during deprotection. This side-reaction takes place next to the electron-rich indolyl moiety and is followed by a subsequent interconversion from the enol form to the keto form due to keto–enol tautomerism. This byproduct is no longer photochromic because of the disruption of the central hexatriene unit. However, it can be clearly distinguished from the mixture (*E*/*Z*)-**1** and pure (*E*)-**1** and (*C*)-**1**, and it is not formed during illumination of the amide-terminated alkyl SAM with the fulgimide headgroup (Supporting Information, Figures S1–S3). The pure isomers (*E*)-**1** and (*Z*)-**1** were applied in an independent study and were derived from the 85:15 mixture of (*E*/*Z*)-**1**.[7] The isomer (*C*)-**1** was obtained in 45% yield by irradiation of the mixture (*E*/*Z*)-**1** at 365 nm (short-arc lamp, Osram HBO, 200 W) in benzene for 24 h, followed by purification by flash chromatography in the dark. Isomer (*C*)-**1** was dissolved in benzene and irradiated at 545 nm (xenon-arc lamp, Osram XBO, 1000 W) for 2 h to yield pure (*E*)-**1**, quantitatively. Photoswitch-linker conjugate (*E*/*Z*)-**7** was synthesized as IR reference substance from undec-10-enoic acid and (*E*/*Z*)-**1** (85:15 mixture) with HCTU in acetonitrile at room temperature within 30 min and was isolated in 96% yield after workup and purification by flash chromatography (Supporting Information, Scheme S1). The ultraviolet–visible spectroscopy (UV/vis) data of the open-isomers [(*E*/*Z*)-mixtures] and the closed-isomers [(*C*)-isomers] of compounds **1**, **5**, **6**, and **7** were measured in benzene at room temperature as previously described[14] and are listed in the Supporting Information (Table S1). The isomer ratios in the PSS at 365 nm (compounds **1**, **5**, **6**, and **7**) and at 545 nm (compound **6**) were determined by reversed-phase high-performance liquid chromatography (RP-HPLC). In comparison to the 1-methyl indolylfulgimides described previously,[14] similar results were obtained here. However, the replacement of the methyl group at the indole nitrogen by a hydrogen atom resulted in an increase of the content of the colored forms [(*C*)-isomers] of compounds **1**, **5**, **6**, and **7** in the PSS at 365 nm to 79–83%.

RESULTS AND DISCUSSION

Preparation of High-Quality, Carboxy-Terminated Alkyl SAMs on Si(111) by Thermal Grafting. Initially, several series of samples were prepared from H-terminated Si(111) and methyl undec-10-enoate using thermal grafting procedures (160 °C, 2 h) in carefully dried and degassed neat reagents.[15] However, it was often not possible to exclude the presence of water and oxygen from the grafting solutions. As a result, we observed the formation of SiO_x and a partial hydrolysis of the ester. Furthermore, it proved to be challenging to obtain reproducible packing densities in the self-assembled monolayer (SAM). Cleavage of the methyl ester-terminated alkyl SAM was first attempted in 2 M hydrochloric acid (HCl) at 70 °C,[15,16] but this method was often accompanied by significant SiO_x formation. Milder conditions were required, and the cleavage was instead performed in 5.5 M HCl (degassed with argon) at 40 °C for 3 h,[17] resulting in a clean conversion of the ester group to the carboxyl group. Finally, all thermal reactions were performed in a closed vessel in a glovebox under nitrogen and anhydrous conditions. This greatly improved the reproducibility and quality of the grafting step, furnishing ester-terminated alkyl SAMs.

The synthetic steps described above were validated by attenuated total reflection Fourier-transform infrared spectroscopy (ATR-FTIR) and X-ray photoelectron spectroscopy (XPS) (see also Supporting Information, Figures S4–S18). Figure 1 shows ATR-FTIR spectra of the ester and acid layer (black and red lines, respectively) grafted on H–Si(111). The spectra are dominated by the ν(C=O) absorption band, which shifts from 1747 cm^{-1} in the ester layer to 1718 cm^{-1} in the acid layer. The cleavage reaction is additionally confirmed by the disappearance of the symmetric and antisymmetric CH_3 absorption bands, $\delta_{sym}(CH_3)$ and $\delta_{as}(CH_3)$, at 1366 and 1438 cm^{-1}, which are observed for the ester but not for the acid layer (Figure 1a). Vice versa, the δ(OH) vibration at 1415 cm^{-1} occurs only for the acid but not for the ester layer.

The ATR-FTIR data in Figure 1b show the alkyl region of the ester- (black line) and carboxy-terminated (red line) SAM with the $\nu_{as}(CH_2)$ and $\nu_{sym}(CH_2)$ absorption at 2924 and 2854 cm^{-1}, respectively.[18] Comparing ester- and acid-termination, these bands only slightly change in wavenumber and intensity, indicating only small conformational changes of the alkyl-linker layer. For example, a different twist of the alkyl chains in the acid-terminated SAM may support the formation of hydrogen bonds among the carboxy end-groups. The shoulder at 2958 cm^{-1} corresponds to the asymmetric $\nu_{as}(CH_3)$ vibration and is, according to this, observed for the ester layer only.

dx.doi.org/10.1021/la402068d | *Langmuir* 2013, 29, 11758–11769

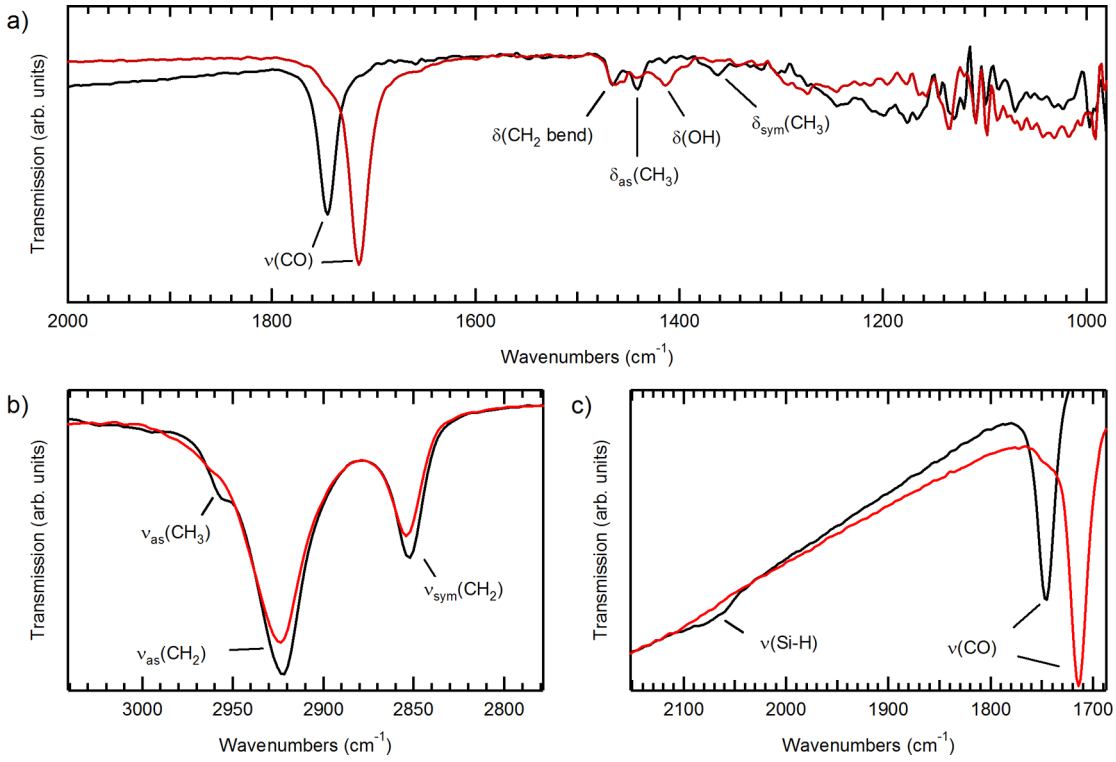

Figure 1. (a) ATR-FTIR spectra of the ester layer (black line) and the acid layer (red line) grafted on H−Si(111). Data are referenced to the spectrum of H−Si(111). (b) Alkyl region with $\nu_{as}(CH_2)$ and $\nu_{sym}(CH_2)$ absorption bands of ester- (black line) and carboxy-terminated (red line) SAMs. (c) Superposition of the ATR-FTIR spectra of the ester- (black line) and acid-terminated alkyl SAM (red line), referenced to the spectrum of SiO_x to resolve the Si−H contribution.

Even in a densely packed alkyl SAM, steric constraints suggest about 50% remaining H-terminated silicon sites. They appear in the ester-terminated SAM when referencing the ATR-FTIR data against SiO_x.[11] As highlighted in Figure 1c, we observed a broad absorption band around 2070 cm^{-1}, which we assign to the unreacted Si−H sites between the grafted alkyl chains.[19] Upon ester cleavage, this band disappeared, accompanied by a slight increase in the 1300−1200 cm^{-1} region (see Figure 1a.). We suggest that these changes originate from hydrolysis of the remaining Si−H bonds between the alkyl chains (vide infra).

In the following, the various synthesis steps are confirmed and further quantified by XPS. The C1s and O1s core-level spectra of the methyl ester-terminated monolayer are shown at the top of Figure 2. The C1s spectrum is dominated by the C_{10} alkyl backbone of the linker, which accounts for the main peak at 284.9 eV. Its asymmetric peak shape is ascribed to the excitation of C−H vibrational modes (2800−3000 cm^{-1} ≈ 0.35−0.37 eV) upon core ionization. Similar asymmetric XPS line shapes were found for SAMs of long-chain alkanethiols chemisorbed on gold and silver.[20] The small shoulder seen at lower binding energy is attributed to the carbon atom directly bound to the silicon surface (Si−C). Its C1s binding energy of 284.0 eV is compatible with those reported for small hydrocarbons chemisorbed on Si(100).[21] The two components at higher binding energies of 287.4 and 289.6 eV can be unambiguously assigned to the C1s core levels of the methoxy and carbonyl groups of the ester, respectively.[24,25] As expected, both components show equal intensity; however, each signal is 1.7 times larger than that of the Si−C surface component because of the dampening by the overlying molecular layer.[26,27]

Corresponding components with equal intensity were also found in the O1s XP spectra of methyl ester-terminated alkyl SAMs (Figure 2b, top). The single- and double-bonded oxygen atoms show chemically shifted XPS lines at 534.2 and 532.7 eV binding energy, respectively.[24,28] The additional shoulder at the low-energy side is attributed to Si−O. The same O1s binding energy of 532.2 eV was observed for the Si−O contaminations at the H-terminated Si(111) surface (Supporting Information, Figure S6).[29]

Upon hydrolysis of the methyl ester end-group, the C1s XPS peak at 287.4 eV, attributed to it, completely disappeared in the spectrum of the carboxy-terminated alkyl SAM (Figure 2a, center). This observation supports the above assignment and, moreover, confirms that the methyl ester cleavage runs till completion. The C1s line of the carbonyl group shifts to a slightly higher binding energy and, in particular, its full width at half-maximum (fwhm) increases by 36%. In line with the small changes of the alkyl vibrations (cf. Figure 1b), we attribute this broadening to the formation of acid pairs via hydrogen bonding, which would also change the intramolecular orientation, i.e., the conformation of the C_{11} alkyl-linker chains. This assumption is corroborated by the shift of the C1s main peak to lower binding energy (284.8 eV) and the increase of its fwhm by 7%. As expected, the surface-bound Si−C component remains at constant binding energy. Cleavage of the methoxy group reduces the peak splitting in the O1s XP spectra to 1.2 eV with the hydroxyl and carboxyl groups at 534.0 and 532.8 eV, respectively. Note that also in case of hydrogen bond formation two chemically shifted XPS components are observed, since on the time scale of the core-level excitation the oxygen atoms remain unequal. Comparison of the C1s and O1s intensities consistently reveals that the ester- and the

dx.doi.org/10.1021/la402068d | Langmuir 2013, 29, 11758−11769

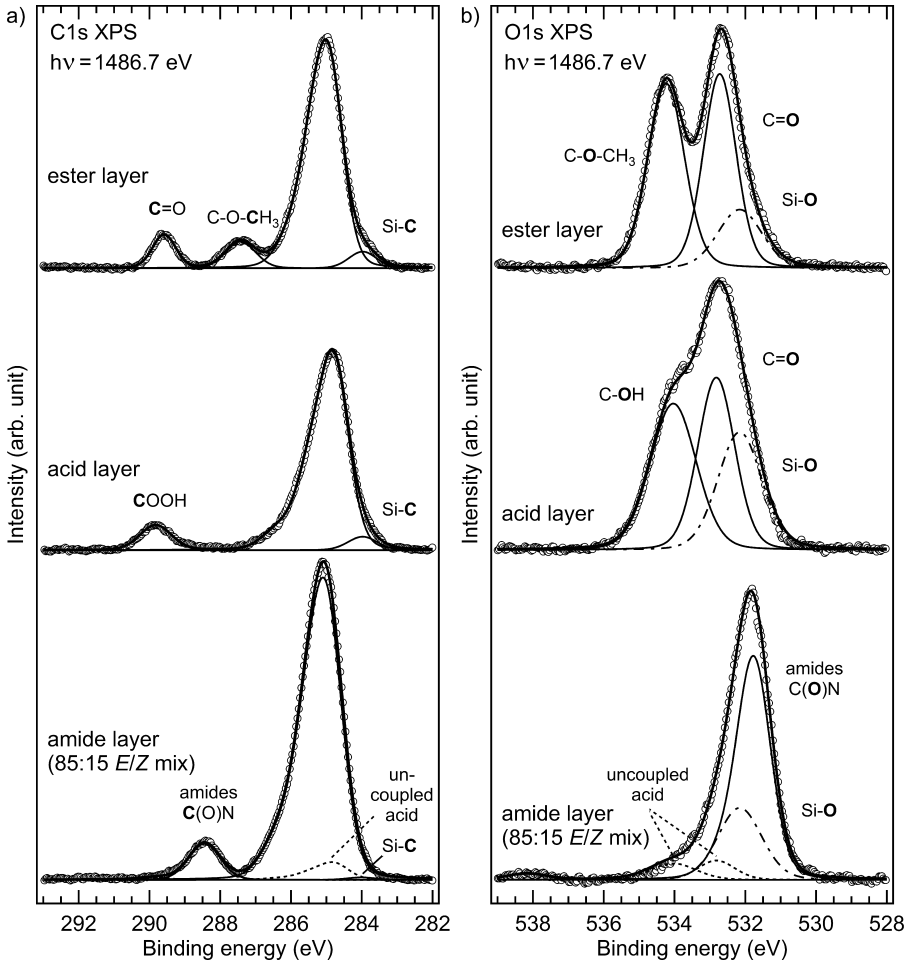

Figure 2. XPS scans of (a) the C1s and (b) the O1s core levels recorded with monochromatized Al KαI radiation ($h\nu$ = 1486.7 eV) at a sample temperature of 300 K. The sequence follows from top to bottom the molecular grafting from the ester, via the acid, to the amide layer containing fulgimide (*E*/*Z*)-**1**.

carboxy-terminated monolayer have comparable coverage. This result supports the existence of an intact monolayer as suggested by ATR-FTIR.

Potential oxidation of the silicon surface during the preparation procedure was monitored by the Si2p core-level spectrum, which exhibits distinct chemical shifts according to the silicon oxidation state. Figure 3 depicts XP spectra of the native silicon oxide surface of n-doped Si(111), the H-terminated Si(111) surface prior to grafting, the methyl ester-terminated monolayer, and the subsequent carboxy- and amide-terminated monolayers. A survey of the binding energies is given in the Supporting Information (Figure S4). The silicon wafer with its native oxide capping layer showed, besides the 2p doublet, the typical silicon oxidation states, Si^{+1}, Si^{+2}, and Si^{+3}, and the dominant Si^{+4} component gradually shifted to higher binding energies.[30] The shift of the Si2p level with respect to H−Si(111) is attributed to surface band bending. The H-terminated surface exhibited none of the higher oxidation states (Si^{+2}, Si^{+3}, or Si^{+4}), revealing the high efficiency of the etching procedure. There was, however, a small, second doublet chemically shifted by 0.90 eV to higher binding energy, which indicated the presence of Si−O, i.e., silicon atoms in oxidation state +1. We note that the Si−O signal was too weak to be detected in normal emission, where the surface sensitivity of the XPS measurement is reduced (see Supporting Information, Figure S5).

After cleavage of the methyl ester, we observed a doubling in intensity of the Si−O component, in both the O1s (Figure 2b) and Si2p (Figure 3) XP spectra. The oxygen XPS peak of Si−O accounts for 28% of the total O1s signal for the carboxy-terminated alkyl SAM (Figure 2b). As we found only Si^{+1} species in the silicon XPS (Figure 3) after the grafting step, remaining H-terminated Si(111) sites must have been replaced by hydroxyl groups, furnishing HO−Si(111). We assume that the O1s signal of these hydroxyl groups is dampened by the overlying densely packed alkyl SAM. Comparing the Si2p signal of H-terminated Si(111) and the carboxy-terminated monolayer in Figure 3, we estimate this dampening to be about 25%. Together, this assessment yields a nearly 1:1 ratio of Si−OH- and Si−C-terminated surface areas. In other words, every second H-terminated site of H−Si(111) carries an alkyl chain, forming a densely packed SAM (Figure 4d).

As an independent proof of the surface coverage, the thickness and electron density of the carboxy-terminated alkyl SAM on Si(111) were determined by X-ray reflectivity (XRR) measurements.[31] Figure 4a shows the offset-corrected specular XRR of a carboxy-terminated alkyl SAM on Si(111) as a function of momentum transfer $q_z = (4\pi/\lambda)\sin(\theta)$, with θ being the angle of incidence. The deviation from the smooth Fresnel reflectivity of the bare Si(111) substrate, i.e., the occurrence of a minimum around 0.22 $Å^{-1}$, gives evidence for a thin layer on top of the silicon. The XRR data were fitted using

dx.doi.org/10.1021/la402068d | *Langmuir* 2013, 29, 11758−11769

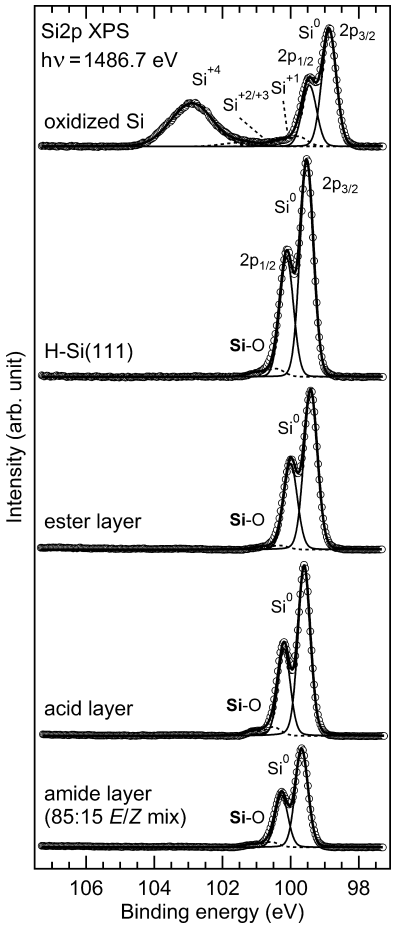

Figure 3. XPS scans of the Si2p core level recorded with monochromatized Al KαI radiation ($h\nu$ = 1486.7 eV) at a sample temperature of 300 K. The sequence starts with the native oxide-capped surface of n-doped silicon, followed by the H-terminated Si(111) surface. The lower three spectra are representative of the on-chip synthesis from the ester-, via the acid-terminated, to the amide-terminated layer using fulgimide (***E/Z***)-**1**.

a stratified homogeneous media approach, where the electron-density distribution along the z-axis is modeled by three slabs (vacuum, SAM, silicon) with smooth boundary conditions.[12] The SAM thickness as obtained from the fit is 14.25 ± 1.0 Å. Assuming a molecular length of ∼16 Å, this thickness corresponds to a molecular tilt angle of 28° ± 8°, which would be in good agreement with measurements of similar SAMs from Sieval et al.[32,33]

The electron density of the monolayer extracted from the fit is 0.30 ± 0.01 e^{-1} $Å^{-3}$. From the values obtained for the thickness (d) and electron density (ρ_e) of the monolayer and the absolute number of electrons per molecule (n_e), one can calculate the surface area per molecule via $A_{mol} = n_e/d\rho_e$. Assuming the presence of both alkyl-linker chains and Si−OH groups, as suggested by XPS, gives an area of 24 ± 2 $Å^2$ per alkyl chain plus hydroxyl group, corresponding to a packing density of (6.8 ± 0.6) × 10^{-10} mol cm^{-2} or (4.1 ± 0.3) × 10^{14} molecules cm^{-2}. Since the maximum theoretical packing density of alkyl chains on Si(111) is 12.8 × 10^{-10} mol cm^{-2}, the XRR results confirm that indeed every second accessible Si bond is occupied by an alkyl chain, in agreement with our XPS data and simulations.[34]

In addition to the out-of-plane information, the in-plane SAM structure, i.e., the spacing d of SAM lattice planes and their epitaxial orientation with respect to the Si(111) surface, was analyzed with grazing incidence X-ray diffraction (GIXD, α_i = 0.18°).[35] Figure 4a shows the azimuthal orientation between silicon and SAM lattice planes as obtained from in-plane Bragg reflections. Besides the Si($2\bar{2}0$) reflection, additional sharp peaks are found that can be assigned to second- and third-order in-plane Bragg reflections of SAM lattice planes that are rotated −30° (for momentum transfer $q_{||}$ = 1.90 ± 0.02 $Å^{-1}$) and +60° (for $q_{||}$ = 2.43 ± 0.02 $Å^{-1}$) with respect to the Si($2\bar{2}0$) planes (see Figure 4b,c). All in-plane reflections of the SAM exhibit a 6-fold rotational symmetry along the azimuthal angle (only one of the six symmetry-equivalent reflections is shown for each $q_{||}$) ascribed to the different SAM domains on the quasihexagonal Si(111) surface. On the basis of the area per molecule and GIXD results, in Figure 4d we show an in-plane unit mesh for the carboxy-terminated alkyl SAM on Si(111) consistent with the derived lattice parameters and azimuthal orientation. The dimensions of the unit mesh are a = 6.65 ± 0.1 Å, b = 7.68 ± 0.1 Å, and β = 90°. Each contains two molecules. According to the mesh parameters, the SAM reflections in Figure 4d are denoted by (20) and (03). The in-plane unit mesh corresponds to a zigzag substitution pattern as proposed in simulations performed by Sieval et al.[32,33] While we use a rectangular primitive unit mesh for indexing the GIXD reflections, the positioning of the alkyl chains with respect to the Si(111) surface atoms can also be described as a c(2 × 4) overlayer (see Figure 4e). No Bragg reflections corresponding to a lattice constant $b' = b/2$ = 3.84 Å resulting from a linear substitution pattern with just one molecule per unit mesh were found.[36] Therefore, a predominant ordering with a zigzag substitution pattern is assumed. From the width Δq of the SAM reflections, we can furthermore estimate the lower limit of the coherent domain size within the SAM via $d_{min} = 2\pi/\Delta q$. In the case of the SAM(20) reflection, this gives a lower limit for the domain width of about 16 nm, i.e., more than 50 lattice planes.

In addition to the carboxy-terminated alkyl SAM, the methyl ester-terminated monolayer was investigated to check for structural changes caused by the ester cleavage. Neither XRR nor GIXD revealed significant structural differences between the ester-terminated and the carboxy-terminated alkyl SAMs (Supporting Information, Figures S7−S9).

Formation of Amide-Terminated Alkyl SAMs by HCTU Coupling. The formation of amide-terminated alkyl SAMs was accomplished by coupling fulgimide (***E/Z***)-**1** (85:15 mixture) to the carboxy-terminated monolayer in a one-step reaction in acetonitrile over a period of 2 h using HCTU[1] and Hünig's base (DIEA, diisopropylethylamine). When the reaction was conducted under oxygen- and water-free conditions in a glovebox, ATR-FTIR showed no byproducts or unreacted reagents and intermediates after workup. The ATR-FTIR signatures of the amide-terminated alkyl SAM on Si(111) (Supporting Information, Figures S10, S17, S18) consist of the characteristic ν_{sym}(C═O) and ν_{as}(C═O) absorption bands due to the imide group of the (*E*/*Z*)-forms of the fulgimide headgroup, which are found at 1739 and 1689 cm^{-1}, respectively. The ν(C═O) amide I band and ν(C−N−H) + δ(C−NH) amide II bands are observed at 1653 and 1544 cm^{-1}, respectively, verifying the formation of the amide-terminated monolayer. The similar $\nu_{as}(CH_2)$ and $\nu_{sym}(CH_2)$ absorption bands of the methyl ester- (black line), carboxy- (red line), and

dx.doi.org/10.1021/la402068d | *Langmuir* 2013, 29, 11758−11769

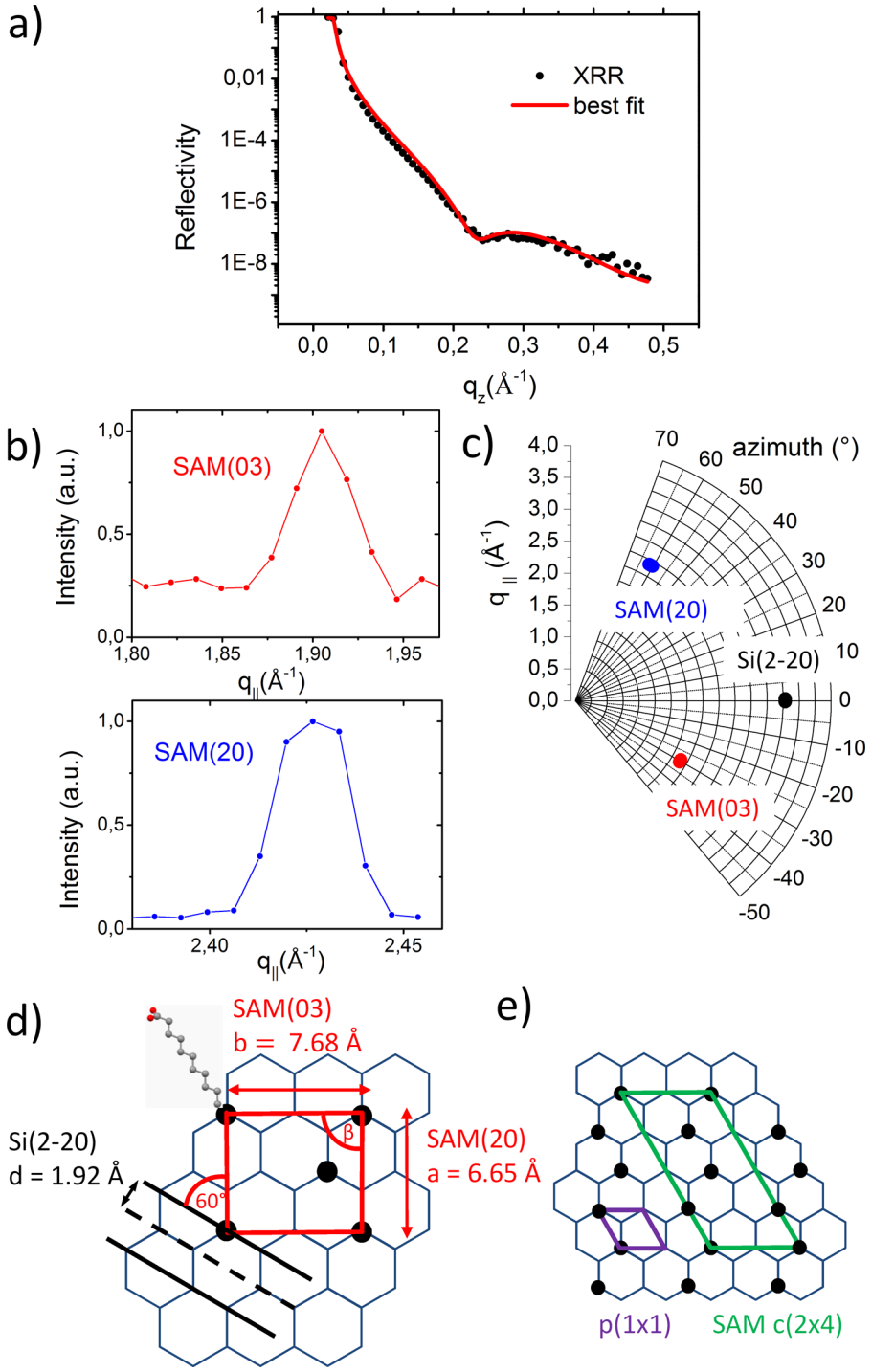

Figure 4. (a) XRR scan of a carboxy-terminated alkyl SAM on Si(111), together with a least-squares fit. The fit gives a total thickness of the layer of d = 14.25 ± 1.0 Å. (b) GIXD scans along $q_{||}$, showing two in-plane Bragg reflections at $q_{||}$ = 1.90 and 2.43 Å^{-1}. (c) Azimuthal distribution of the lattice planes, derived from Bragg reflections in GIXD. (d) Sketch of the in-plane unit mesh with the dimensions a = 6.65 Å, b = 7.68 Å, and β = 90°, containing two molecules (black circles). Blue hexagons depict the Si(111) surface while black lines stand for crystal lattice planes of the Si(2$\bar{2}$0) reflection. (e) Sketch showing the alternative c(2 × 4) description of the SAM unit mesh with respect to the primitive unit mesh of the Si(111) surface atoms.

amide-terminated (blue line) SAMs prove their chemical stability and indicate a dense packing.

In the C1s XP spectra of the amide layer in Figure 2a (bottom), the main peak shifted to a higher binding energy of 285.1 eV, typical for combinations of aromatic and saturated entities, i.e., the fulgimide photoswitch and the alkyl-linker layer. We note that in SAMs comprised of molecules with hybrid aliphatic−aromatic backbone one cannot distinguish between the C1s emission stemming from the aromatic part of the backbone and that originating from the aliphatic part.[22,23] As the concept of the chemical shift is not fully applicable to the photoemission spectra of SAMs, we refrain from further decomposition of the main line. The additional C1s component at a binding energy of 288.4 eV is characteristic for the CONH

dx.doi.org/10.1021/la402068d | Langmuir 2013, 29, 11758−11769

moiety.[37,38] This group shows a larger signal than the carboxyl group of the acid layer, reflecting the additional imide group of the fulgimide.

The O1s main peak of the amide layer in Figure 2b (bottom) strongly shifted to a lower binding energy of 531.8 eV, compatible with the literature value for an amide-terminated alkyl SAM.[37] To properly fit the O1s XP spectrum, we needed, in addition to the Si−O signal, two small components representing some remaining, uncoupled carboxyl groups of the carboxy-terminated alkyl-linker SAM. From steric constraints, i.e., considering the respective van der Waals radii, it is obvious that at most only every second carboxy linker can carry a fulgimide molecule (cf. Scheme 2). However, when transferring the peak positions of the hydroxyl and carboxyl groups from the acid layer, the intensity of the uncoupled components in the amide layer amounts to only 11% compared to the acid layer. We conclude that the XPS signal of the uncoupled components is strongly attenuated by the overlaying fulgimide molecules. A similarly strong dampening is seen for the C1s peak of the carboxyl group at 289.8 eV, which renders the C1s signal of the amide and imide groups at 288.4 eV slightly asymmetric.

The strong reduction of the XPS signals of the remaining, uncoupled carboxy-linker molecules upon amide formation with fulgimide (*E*/*Z*)-**1** indicates a dense packing of the photoswitches coupled to the SAM. The C1s signal at the bottom in Figure 2a is larger by a factor of ∼1.6 when comparing the acid- and amide-layer spectrum. Switch and linker contain 20 and 11 carbon atoms, respectively. If we neglected the attenuation of the XPS signal in the molecular layer, we would conclude that every third alkyl linker carries a fulgimide photoswitch: (20/3 + 11)/11 = 1.6. However, as seen from the intensity of the Si2p core level in Figure 3, the dampening of the substrate signal by the aromatic amide-terminated monolayer is about twice as strong as that by the aliphatic alkyl-based monolayers, i.e., the methyl ester-terminated and the carboxy-terminated alkyl SAMs. From the carboxy- to the amide-terminated monolayer, the Si2p signal is reduced by a factor of ∼0.6. Assuming an equal damping of the C1s signal of the alkyl chain, an even denser packing of the fulgimide headgroups on top of the carboxy-terminated monolayer is required to explain the XPS intensities. In fact, the C1s XPS signal of the amide-terminated monolayer requires ∼0.55 fulgimide molecules per carboxy linker: (0.55 × 20 + 0.6 × 11)/11 = 1.6. In conclusion, evaluation of the XPS intensities reveals a high turnover for the amide coupling; on average, one fulgimide photoswitch is coupled to every second alkyl linker.

Combining the results from ATR-FTIR, XPS, and X-ray scattering, we can now deduce reliable models of the various molecular layers. As sketched in Scheme 2, the rectangular unit mesh (a = 6.65 Å, b = 7.68 Å) of the ester and acid layer contains two linker molecules in a zigzag arrangement with a coverage of about 4 × 10^{14} molecules cm^{-2} [∼50% of initially H-terminated Si(111) sites]. The cleavage of the ester runs till completion. During this reaction, hydrolysis of the remaining H−Si(111) sites leads to HO−Si(111) groups between the molecular rows. There is no further, significant oxidation of the silicon substrate. The final one-step reaction using HCTU and Hünig's base leads to a densely packed functionalized SAM with one fulgimide photoswitch per two alkyl-linker molecules, i.e., 2 × 10^{14} molecules cm^{-2} [∼25% of initially H-terminated Si(111) sites].

Readout of the Amide-Terminated Alkyl SAM Using Light. The photoswitching between the mixture of the open (*Z*)- and (*E*)-forms and the closed (*C*)-form with ultraviolet (UV) and visible (vis) light is illustrated in Scheme 3. We note that in solution the ratio between (*Z*)- and (*E*)-forms is identical in both photostationary states (PSS), PSS(365 nm) and PSS(545 nm) (Supporting Information, Table S1). Therefore, IR and UV/vis difference spectra solely monitor the *E*/*Z*-to-*C* and *C*-to-*E*/*Z* conversion upon UV and visible light illumination.[9,10] The switching characteristics of the

Scheme 2. Top and Side Views of the H-Terminated Si(111) Surface, the Grafted Carboxy-Terminated Alkyl-Linker Layer, and the SAM with Coupled Fulgimide Photoswitches[a]

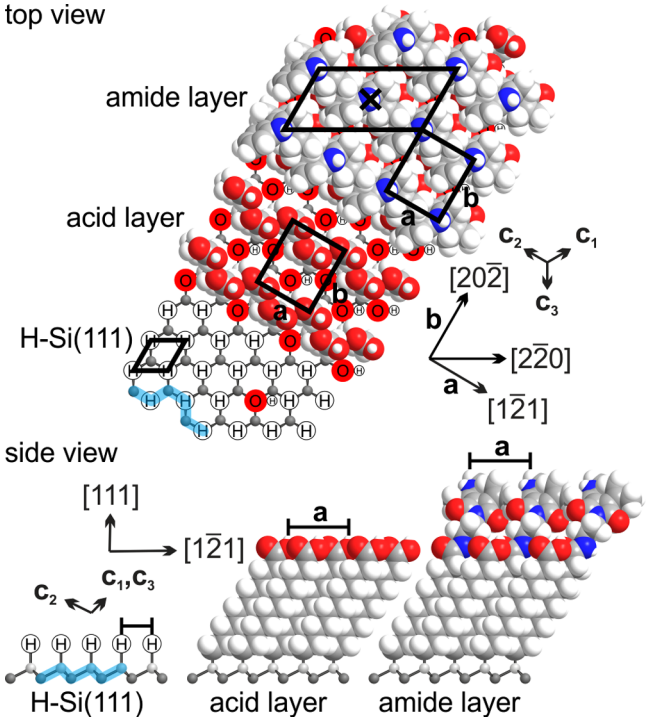

[a]The hard-sphere models of the molecules indicate the van der Waals radii; O and N atoms are shown in red and blue. The primitive unit meshes of H−Si(111) and the acid and amide layer are shown as well as the unit mesh with c(2 × 4) periodicity. The on-chip synthesis leads to a densely packed SAM. The molecular arrangement and surface coverage are deduced combining X-ray scattering, XPS, and ATR-FTIR results.

Scheme 3. Fulgimide Photochromic Equilibria upon Light Illumination with UV (365 nm) and Visible (Vis) Light (545 nm)

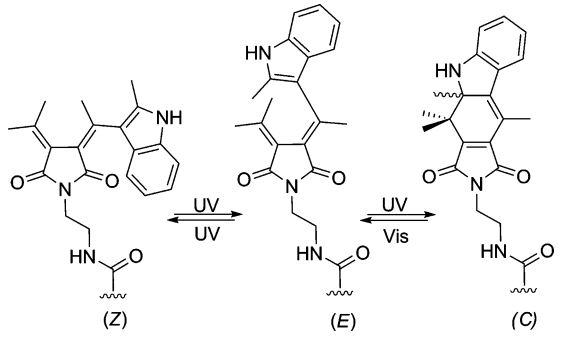

dx.doi.org/10.1021/la402068d | Langmuir 2013, 29, 11758−11769

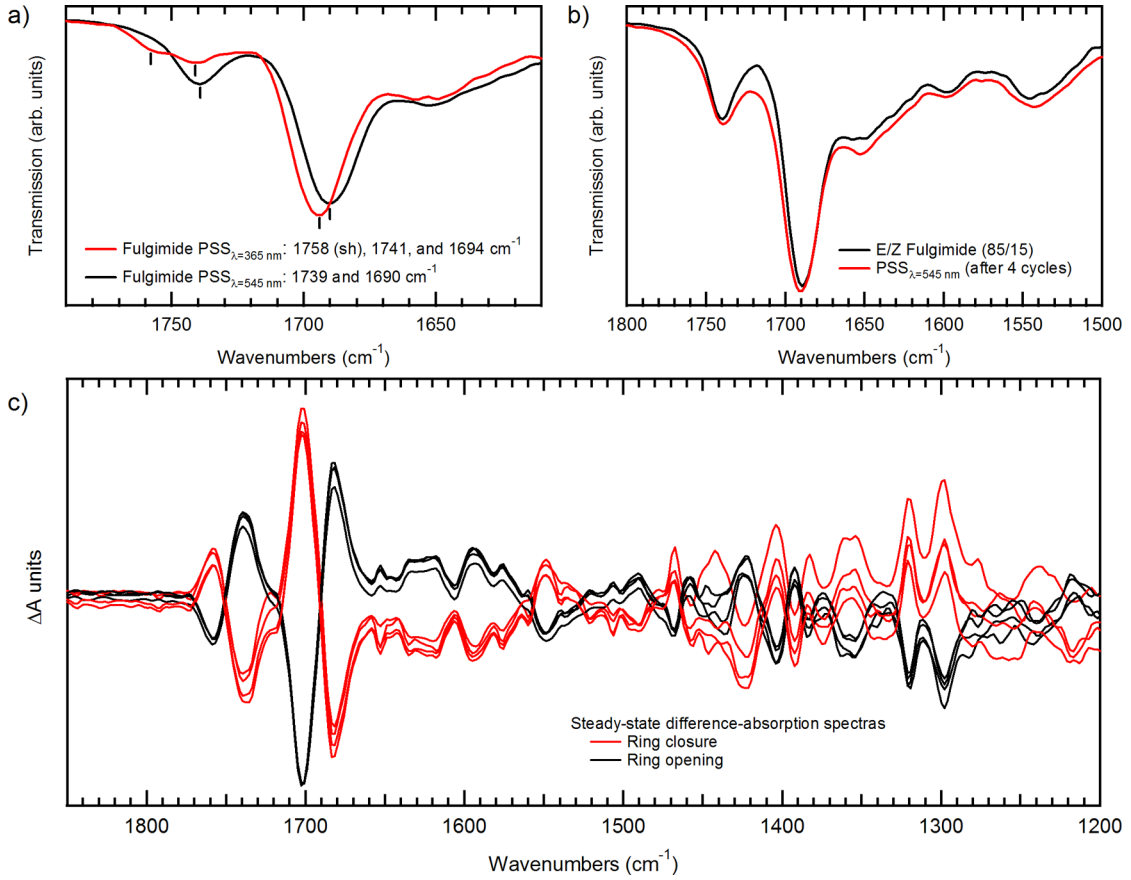

Figure 5. (a) Switching between PSS(365 nm), enriched in the (*C*)-form (red line), and PSS(545 nm), enriched in the (*E*/*Z*)-form of fulgimide **1** (black line). The ATR-FTIR spectra differ in the characteristic ν_{sym}(C═O) and ν_{as}(C═O) absorption bands for the imide moiety of the open and closed fulgimide headgroup. (b) ATR-FTIR spectra of the amide-terminated monolayer derived from fulgimide (***E*/*Z*)-1** (black) and of the PSS(545 nm) after four illumination cycles (red). (c) Steady-state difference-absorption spectra between the photostationary states due to the ring-closure (red) and ring-opening (black) reactions.

amide-terminated SAM bearing the fulgimide headgroup were evaluated by alternating irradiation with UV and visible light and nondestructive readout of the two photostationary states using ATR-FTIR and XPS.

As seen from the ATR-FTIR spectra in Figure 5a, upon irradiation of the amide-terminated monolayer, derived from fulgimide (***E*/*Z*)-1** (85:15 mixture), with 365 nm light, in the PSS(365 nm) the characteristic ν_{sym}(C═O) and ν_{as}(C═O) absorption bands of the (*E*/*Z*)-mixture shifted from 1739 to 1758 cm^{-1} and from 1689 to 1694 cm^{-1}, respectively. In accordance to our IR spectroscopy studies in solution (Supporting Information, Figure S1), these changes indicate the ring-closure of the (*E*)-fulgimide to the (*C*)-fulgimide and the arrival at a PSS(365 nm) enriched in the (*C*)-form. Comparable to the situation in solution, switching between the (*E*)- and the (*Z*)-form in the SAM is not detectable by IR spectroscopy. Upon irradiation with 545 nm light, a PSS(545 nm) containing the (*E*)- and (*Z*)-forms is reached, and the ν_{sym}(C═O) and ν_{as}(C═O) absorption bands shift back to 1739 and 1690 cm^{-1}, respectively.

In Figure 5b, the ATR-FTIR spectrum of the amide-terminated alkyl SAM derived from fulgimide (***E*/*Z*)-1** (85:15 mixture) is superimposed with the ATR-FTIR spectrum of the photostationary state PSS(545 nm) after four illumination cycles. This comparison indicates a nearly fully reversible switching behavior. As illustrated in Figure 5c for four irradiation cycles, the steady-state difference spectra between the photostationary states PSS(365 nm) and PSS(545 nm) of the fulgimide headgroup due to the ring-closing and ring-opening reactions remained nearly unchanged.

XPS measurements confirm the expected (*E*/*Z*)-to-(*C*) ring closure for reaching PSS(365 nm). Subsequent (*C*)-to-(*E*/*Z*) ring-opening, furnishing PSS(545 nm), as well as successive ring-closing and -opening cycles all led to weak but clearly discernible changes in the recorded spectra. The N1s and C1s signals of the fulgimide layer's imide and amide groups are depicted in Figure 6a,b. The oxidation of the Si surface, traced by the Si^{+1} 2p XPS component, increased only slightly after the first irradiation. However, even though greatest care was taken, a continuous, minor buildup in the carbon and oxygen spectra's main peaks was observed and attributed to contaminants. Therefore, switching of XPS samples was stopped after two cycles each.

The changes of the N1s and C1s peak heights and peak widths as well as the C1s binding energy of the amide/imide moiety upon irradiation are summarized in Figure 6c,d. As mentioned in the Experimental Section, the latter was determined by fitting the C1s spectra after subtracting all other peaks (see Figure S20 in the Supporting Information). Analogously to the ATR-FTIR data, the XPS measurements show that the original 85:15 ratio of the starting (*E*/*Z*)-mixture was not fully reached after the first irradiation cycle, but only minor variations were observed. On the molecular level, ring-closing and -opening reactions are affecting the indolyl ring

dx.doi.org/10.1021/la402068d | *Langmuir* 2013, 29, 11758−11769

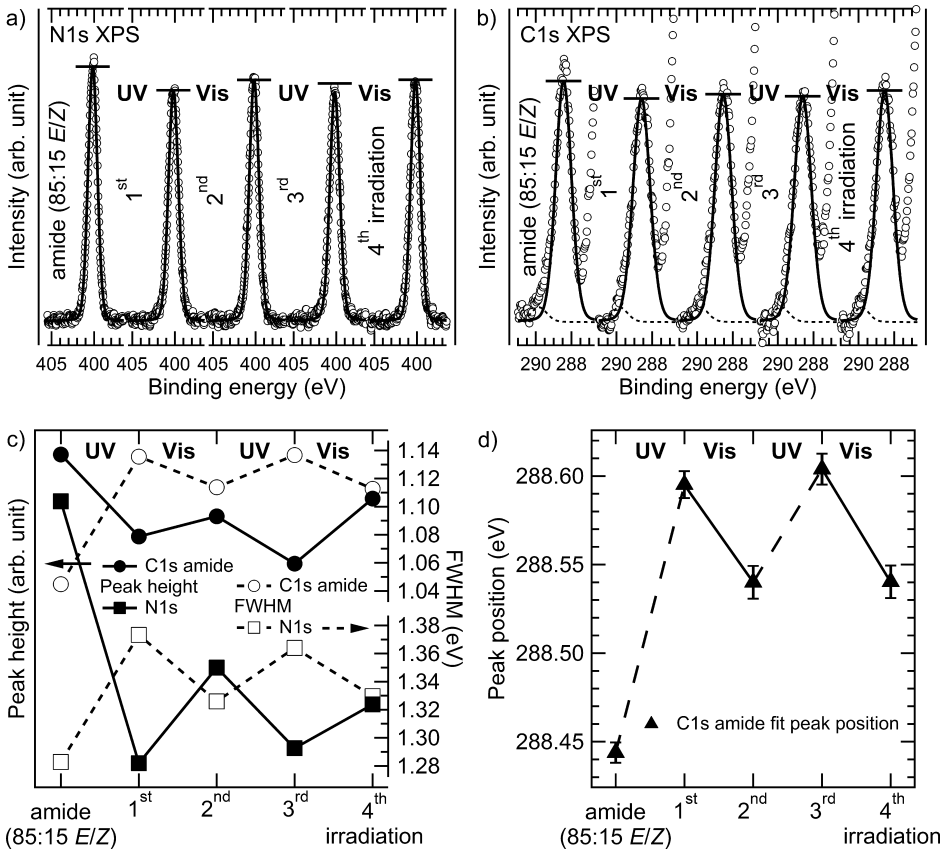

Figure 6. XP spectra of (a) the N1s and (b) the C1s core-level components of the pristine amide-terminated monolayer bearing fulgimide moieties and two alternating irradiation cycles at wavelengths of 365 and 545 nm, respectively. (c) N1s and C1s peak heights and widths and (d) binding energy of the C1s core level of the amide/imide moiety extracted from parts a and b. The weak oscillations of all signals demonstrate two iterative cycles of switching and back-switching of the fulgimide SAM with UV (365 nm) and vis (545 nm) light, respectively.

with its embedded nitrogen atom. Ring-closure of the (*E*)-form, containing a helical hexatriene system with an intact indole ring, furnishes the planar, conjugated ring-closed (*C*)-form with its cyclohexadiene core structure containing two sp^3-hybridized carbon atoms.

Because of these structural variations in the respective nitrogen atom's chemical surrounding, changes in the recorded N1s spectra in a breathing-like fashion were observed, as shown in Figure 6c. The N1s peak height (filled squares) is clearly reduced after the first irradiation with UV light (365 nm) and weakly increases and decreases after each following irradiation session with visible (545 nm) and UV light, respectively. The peak's fwhm varies in the opposite manner, beginning with a small width that is first increased and then slightly decreased and increased again (open squares in Figure 6c). Analogously, in the carbon spectra the modified environment causes the amide signal to breathe as well. This peak not only varies in height and width (filled and open circles in Figure 6c) but also changes its binding energy peak position by about 50 meV (Figure 6d and Figure S20 in the Supporting Information). We attribute the small but reversible changes of the XP spectra to the repeated ring-closing and -opening cycles due to the associated structural alterations described above and, accordingly, the corresponding changes in bulk properties.

Both ATR-FTIR and XPS demonstrate reversible photoswitching of the fulgimide SAM. The photostationary states are reached after irradiating the SAM with about 10^{19} photons cm^{-2} in the UV or vis range (2 and 5 mW for 30 min). Assuming a photostationary state PSS(365 nm) consisting of 70% of the (*C*)-isomer, i.e., comparable to the molecule in solution, these exposures correspond to large cross sections and demonstrate efficient decoupling of the fulgimide photoswitch from the silicon substrate in the SAM.

■ CONCLUSION

We prepared densely packed ester-terminated alkyl self-assembled monolayers on Si(111) by thermal grafting in a glovebox and subsequently hydrolyzed the methyl ester to give an acid end-group, while simultaneously the remaining H–Si(111) sites were hydrolyzed to HO–Si(111). X-ray photoelectron spectroscopy and X-ray reflectivity measurements indicate a surface coverage of about 50% for the carboxy-terminated alkyl SAM [with respect to the H-terminated sites of H–Si(111)] while grazing incidence X-ray diffraction results imply a unit mesh with a regular zigzag-like substitution pattern (Figure 4d and Scheme 2). The coverage corresponds to a densely packed alkyl SAM. The amounts of alkyl linkers and hydroxyl groups after thermal grafting and subsequent hydrolysis of the ester end-group are similar, thereby indicating a well-defined, neat carboxy-terminated alkyl SAM. The aminium-based coupling reagent HCTU[1] gave, under one-pot coupling conditions, high-quality, amide-terminated alkyl SAMs with a fulgimide headgroup. Since the fulgimide is quite voluminous compared to the packing density of the carboxyl groups in the linker layer, a maximum coupling yield of 50% is possible, i.e., every second carboxy linker carries a fulgimide

dx.doi.org/10.1021/la402068d | *Langmuir* 2013, 29, 11758–11769

(Scheme 2). Photoswitching between the two photostationary states, PSS(365 nm) and PSS(545 nm), is observed with a fluence of less than 10 J cm^{-2}. This corresponds to high cross sections of 10^{-19} cm^2, suitable for practical applications.

■ ASSOCIATED CONTENT

Ⓢ Supporting Information

Experimental data (synthesis), additional ATR-FTIR data, XPS data, and XRR data. This material is available free of charge via the Internet at http://pubs.acs.org.

■ AUTHOR INFORMATION

Corresponding Authors

*K.R.-B.: e-mail, karola.rueck-braun@tu-berlin.de.
*M.W.: e-mail, weinelt@physik.fu-berlin.de.

Present Addresses

[‖]Department of Chemistry, Technical University of Denmark, DK-2800 Kgs.-Lyngby, Denmark.
[⊥]Chemistry Department, Faculty of Applied Sciences, Umm-Al-Qura University, 21955 Makkah, KSA.

Notes

The authors declare no competing financial interest.

■ ACKNOWLEDGMENTS

The SFB 658 ("Elementary Processes in Molecular Switches at Surfaces"), the Fonds der Chemischen Industrie, The Danish Research Council for Independent Research | Natural Sciences, The Carlsberg Foundation, and the Alexander von Humboldt Foundation are gratefully acknowledged for supporting this work.

■ REFERENCES

(1) HCTU, 2-(6-chloro-1*H*-benzotriazol-1-yl)-1,1,3,3-tetramethyluronium hexafluorophosphate; HBTU, 2-(1*H*-benzotriazol-1-yl)-1,1,3,3-tetramethyluronium hexafluorophosphate.

(2) Shirahata, N.; Hozumi, A.; Yonezawa, T. Monolayer-Derivative Functionalization of Non-Oxidized Silicon Surfaces. *Chem. Rec.* **2005**, *5*, 145−149.

(3) Aswal, D. K.; Lenfant, S.; Guerin, D.; Yakhmi, J. V.; Vuillaume, D. Self Assembled Monolayers on Silicon for Molecular Electronics. *Anal. Chim. Acta* **2006**, *568*, 84−108.

(4) Wayner, D. D. M.; Wolkow, R. A. Organic Modification of Hydrogen Terminated Silicon Surfaces. *J. Chem. Soc., Perkin Trans. 2* **2002**, *1*, 23−34.

(5) Ciampi, S.; Harper, J. B.; Gooding, J. J. Wet Chemical Routes to the Assembly of Organic Monolayers on Silicon Surfaces via the Formation of Si−C Bonds: Surface Preparation, Passivation and Functionalization. *Chem. Soc. Rev.* **2010**, *39*, 2158−2183.

(6) Chazalviel, J.-N.; Allongue, P.; Gouget-Laemmel, A. C.; Henry de Villeneuve, C.; Moraillon, A.; Ozanam, F. Covalent Functionalizations of Silicon Surfaces and Their Application to Biosensors. *Sci. Adv. Mater.* **2011**, *3*, 332−353.

(7) Henry de Villeneuve, C.; Michalik, F.; Chazalviel, J.-N.; Rück-Braun, K.; Allongue, P. Quantitative IR Readout of Fulgimide Monolayer Switching on Si(111) Surfaces. *Adv. Mater.* **2013**, *25*, 416−421.

(8) Rück-Braun, K.; Kempa, S.; Priewisch, B.; Richter, A.; Seedorff, S.; Wallach, L. Azobenzene-Based *ω*-Amino Acids and Related Building Blocks: Synthesis, Properties, and Application in Peptide Chemistry. *Synthesis* **2009**, *24*, 4256−4267.

(9) Koller, F. O.; Schreier, W. J.; Schrader, T. E.; Sieg, A.; Malkmus, S.; Schulz, C.; Dietrich, S.; Rück-Braun, K.; Zinth, W.; Braun, M. Ultrafast Structural Dynamics of Photochromic Indolylfulgimides Studied by Vibrational Spectroscopy and DFT Calculations. *J. Phys. Chem. A* **2006**, *110*, 12769−12776.

(10) Koller, F. O.; Schreier, W. J.; Schrader, T. E.; Malkmus, S.; Schulz, C.; Dietrich, S.; Rück-Braun, K.; Braun, M. Ultrafast Ring-Closure Reaction of Photochromic Indolylfulgimides Studied with UV-Pump-IR-Probe Spectroscopy. *J. Phys. Chem. A* **2008**, *112*, 210−214.

(11) Faucheux, A.; Gouget-Laemmel, A. C.; Henry de Villeneuve, C.; Boukherroub, R.; Ozanam, F.; Allongue, P.; Chazalviel, J.-N. Well-Defined Carboxyl-Terminated Alkyl Monolayers Grafted onto H−Si(111): Packing Density from a Combined AFM and Quantitative IR Study. *Langmuir* **2006**, *22*, 153−162.

(12) Parratt, L. G. Surface Studies of Solids by Total Reflection of X-rays. *Phys. Rev.* **1954**, *95*, 359−369.

(13) Yokoyama, Y.; Takahashi, K. Trifluoromethyl-Substituted Photochromic Indolylfulgide. A Remarkably Durable Fulgide Towards Photochemical and Thermal Treatments. *Chem. Lett.* **1996**, *25*, 1037−1038.

(14) Zarwell, S.; Dietrich, S.; Schulz, C.; Dietrich, P.; Michalik, F.; Rück-Braun, K. Preparation of an Indolylfulgimide-Adamantane Linker Conjugate with Nitrile Anchoring Groups through Palladium-Catalyzed Transformations. *Eur. J. Org. Chem.* **2009**, *13*, 2088−2095.

(15) Dietrich, P.; Michalik, F.; Schmidt, R.; Gahl, C.; Mao, G.; Breusing, M.; Raschke, M. B.; Priewisch, B.; Elsässer, T.; Mendelsohn, R.; Weinelt, M.; Rück-Braun, K. An Anchoring Strategy for Photoswitchable Biosensor Technology: Azobenzene-Modified SAMs on Si(111). *Appl. Phys. A* **2008**, *93*, 285−292.

(16) Boukherroub, R.; Wayner, D. D. M. Controlled Functionalization and Multistep Chemical Manipulation of Covalently Modified Si(111) Surfaces. *J. Am. Chem. Soc.* **1999**, *121*, 11513−11515.

(17) Touahir, L.; Chazalviel, J.-N.; Sam, S.; Moraillon, A.; Henry de Villeneuve, C.; Allongue, P.; Ozanam, F.; Gouget-Laemmel, A. C. Kinetics of Activation of Carboxyls to Succinimidyl Ester Groups in Monolayers Grafted on Silicon: An in Situ Real-Time Infrared Spectroscopy Study. *J. Phys. Chem. C* **2011**, *115*, 6782−6787.

(18) Porter, M. D.; Bright, T. B.; Allara, D. L.; Chidsey, C. E. D. Spontaneously Organized Molecular Assemblies. 4. Structural Characterization of *n*-Alkyl Thiol Monolayers on Gold by Optical Ellipsometry, Infrared Spectroscopy, and Electrochemistry. *J. Am. Chem. Soc.* **1987**, *109*, 3559−3568.

(19) Raghavachari, K.; Jakob, P.; Chabal, Y. J. Step Relaxation and Surface Stress at H-Terminated Vicinal Si(111). *Chem. Phys. Lett.* **1993**, *206*, 156−160.

(20) Heister, K.; Johansson, L. S. O.; Grunze, M.; Zharnikov, M. A Detailed Analysis of the C 1s Photoemission of *n*-Alkanethiolate Films on Noble Metal Substrates. *Surf. Sci.* **2003**, *529*, 36−46.

(21) Fink, A.; Widdra, W.; Wurth, W.; Keller, C.; Stichler, M.; Achleitner, A.; Comelli, G.; Lizzit, S.; Baraldi, A.; Menzel, D. Core-Level Spectroscopy of Hydrocarbons Adsorbed on Si(100)-(2 × 1): A Systematic Comparison. *Phys. Rev. B* **2001**, *64*, 045308.

(22) Heister, K.; Rong, H.-T.; Buck, M.; Zharnikov, M.; Grunze, M.; Johansson, L. S. O. Odd−Even Effects at the S−Metal Interface and in the Aromatic Matrix of Biphenyl-Substituted Alkanethiol Self-Assembled Monolayers. *J. Phys. Chem. B* **2001**, *105*, 6888−6894.

(23) Shaporenko, A.; Brunnbauer, M.; Terfort, A.; Grunze, M.; Zharnikov, M. Structural Forces in Self-Assembled Monolayers: Terphenyl-Substituted Alkanethiols on Noble Metal Substrates. *J. Phys. Chem. B* **2004**, *108*, 14462−14469.

(24) Whelan, C. M.; Ghijsen, J.; Pireaux, J.-J.; Maex, K. Cu Adsorption on Carboxylic Acid-Terminated Self-Assembled Monolayers: A High-Resolution X-ray Photoelectron Spectroscopy Study. *Thin Solid Films* **2004**, *464−465*, 388−392.

(25) Zubavichus, Y.; Fuchs, O.; Weinhardt, L.; Heske, C.; Umbach, E.; Denlinger, J. D.; Grunze, M. Soft X-ray-Induced Decomposition of Amino Acids: An XPS, Mass Spectrometry, and NEXAFS Study. *Radiat. Res.* **2004**, *161*, 346−358.

(26) Lamont, C. L. A.; Wilkes, J. Attenuation Length of Electrons in Self-Assembled Monolayers of *n*-Alkanethiols on Gold. *Langmuir* **1999**, *15*, 2037−2042.

(27) Schmidt, R.; McNellis, E.; Freyer, W.; Brete, D.; Gießel, T.; Gahl, C.; Reuter, K.; Weinelt, M. Azobenzene-Functionalized

Alkanethiols in Self-Assembled Monolayers on Gold. *Appl. Phys. A* **2008**, *93*, 267−275.
(28) Ketteler, G.; Ashby, P.; Mun, B. S.; Ratera, I.; Bluhm, H.; Kasemo, B.; Salmeron, M. In situ Photoelectron Spectroscopy Study of Water Adsorption on Model Biomaterial Surfaces. *J. Phys.: Condens. Matter* **2008**, *20*, 184024.
(29) Popoff, R. T. W.; Asanuma, H.; Yu, H.-Z. Long-Term Stability and Electrical Performance of Organic Monolayers on Hydrogen-Terminated Silicon. *J. Phys. Chem. C* **2010**, *114*, 10866−10872.
(30) Dreiner, S.; Schürmann, M.; Westphal, C.; Zacharias, H. Local Atomic Environment of Si Suboxides at the SiO_2/Si(111) Interface Determined by Angle-Scanned Photoelectron Diffraction. *Phys. Rev. Lett.* **2001**, *86*, 4068−4071.
(31) Tolan, M. *X-ray Scattering from Soft-Matter Thin Films: Materials Science and Basic Research*; Springer Tracts in Modern Physics; Springer: Berlin, 1999 ; Vol. *148*.
(32) Sieval, A. B.; van den Hout, B.; Zuilhof, H.; Sudhölter, E. J. R. Molecular Modeling of Alkyl Monolayers on the Si(111) Surface. *Langmuir* **2000**, *16*, 2987−2990.
(33) Sieval, A. B.; van den Hout, B.; Zuilhof, H.; Sudhölter, E. J. R. Molecular Modeling on Covalently Attached Alkyl Monolayers on the Hydrogen-Terminated Si(111) Surface. *Langmuir* **2001**, *17*, 2172−2181.
(34) Gorostiza, P.; Henry de Villeneuve, C.; Sun, Q. Y.; Sanz, F.; Wallart, X.; Boukherroub, R.; Allongue, P. Water Exclusion at the Nanometer Scale Provides Long-Term Passivation of Silicon (111) Grafted with Alkyl Monolayers. *J. Phys. Chem. B* **2006**, *110*, 5576−5585.
(35) Als-Nielsen, J.; McMorrow, D. *Elements of Modern X-ray Physics*; John Wiley & Sons: Chichester, U.K., 2001.
(36) Linford, M. R.; Fenter, P.; Eisenberger, P. M.; Chidsey, C. E. D. Alkyl Monolayers on Silicon Prepared from 1-Alkenes and Hydrogen-Terminated Silicon. *J. Am. Chem. Soc.* **1995**, *117*, 3145−3155.
(37) Hooper, A. E.; Werho, D.; Hopson, T.; Palmer, O. Evaluation of Amine- And Amide-Terminated Self-Assembled Monolayers as 'Molecular Glues' for Au and SiO_2 Substrates. *Surf. Interface Anal.* **2001**, *31*, 809−814.
(38) Whelan, C. M.; Cecchet, F.; Baxter, R.; Zerbetto, F.; Clarkson, G. J.; Leigh, D. A.; Rudolf, P. Adsorption of a Benzylic Amide Macrocycle on a Solid Substrate: XPS and HREELS Characterization of Thin Films Grown on Au(111). *J. Phys. Chem. B* **2002**, *106*, 8739−8746.